Kondo behavior and conductance through 3d impurities in gold chains doped with oxygen

M. A. Barral, S. Di Napoli, G. Blesio, P. Roura-Bas, A. Camjayi, L. O. Manuel, and A. A. Aligia

Kondo behavior and conductance through 3*d* impurities in gold chains doped with oxygen

M. A. Barral,[1] S. Di Napoli,[1] G. Blesio,[2] P. Roura-Bas,[1] A. Camjayi,[3] L. O. Manuel,[2] and A. A. Aligia[4]

[1]*Dpto de Física de la Materia Condensada, GIyA-CNEA, Avenida General Paz 1499, 1650 San Martín, Provincia de Buenos Aires, Argentina and CONICET, 1033 CABA, Argentina*
[2]*Instituto de Física Rosario, Facultad de Ciencias Exactas, Ingeniería y Agrimensura, Universidad Nacional de Rosario, CONICET, Bv. 27 de Febrero 210 bis, 2000 Rosario, Argentina*
[3]*Departamento de Física, FCEyN, Universidad de Buenos Aires and IFIBA, Pabellón I, Ciudad Universitaria, CONICET, 1428 CABA, Argentina*
[4]*Centro Atómico Bariloche and Instituto Balseiro, Comisión Nacional de Energía Atómica, CONICET, 8400 Bariloche, Argentina*

Combining *ab initio* calculations and effective models derived from them, we discuss the electronic structure of oxygen doped gold chains when one Au atom is replaced by any transition-metal atom of the 3*d* series. The effect of O doping is to bring extended Au $5d_{xz}$ and $5d_{yz}$ states to the Fermi level, which together with the Au states of zero angular momentum projection leads to three possible channels for the screening of the magnetism of the impurity. For most 3*d* impurities the expected physics is similar to that of the underscreened Kondo model, with singular Fermi liquid behavior. For Fe and Co under a tetragonal crystal field introduced by leads, the system might display a non-Fermi liquid behavior. Ni and Cu impurities are described by a $S = 1$ two channel Kondo model and an SU(4) impurity Anderson model in the intermediate valence regime, respectively. In both cases, the system is a Fermi liquid, but the conductance shows some observable differences with the ordinary SU(2) Anderson model. *Published by AIP Publishing.* [http://dx.doi.org/10.1063/1.4973982]

I. INTRODUCTION

In the last years, there has been a great amount of experiments in electronic transport through semiconducting[1–7] and molecular[8–12] quantum dots (QDs), in which manifestations of the Kondo effect were observed. In addition, experiments with mechanically controllable break junctions made possible to create one-dimensional atomic chains of several elements,[13–15] and the conductance of noble-metal nanowires with transition-metals impurities has been measured using point-contact techniques.[16,17]

The Kondo effect is one of the paradigms in strongly correlated condensed matter systems[18] and arises when the spin of a localized electron (such as that of a magnetic 3*d* impurity) is at least partially screened by conduction electrons interacting with the spin. The Kondo model, in its simplest version, consists of a spin 1/2 with an exchange interaction with a single conduction band. The localized spin and the conduction electrons form a many-body singlet ground state. The binding energy of this singlet is of the order of the characteristic Kondo temperature T_K below which the effects of the "screening" of the impurity spin manifest themselves in different physical properties, such as the conductance as a function of temperature $G(T)$, which has been measured in quantum dots and is in excellent agreement with theory.[5]

In the general case, the localized spin has magnitude S and can be screened by N channels, which correspond to conduction states of different symmetry. The case $2S = N$ (including the simplest one $2S = N = 1$) corresponds to the *fully screened* case with a singlet ground state. For $2S > N$ one has the *underscreened case*, in which the total spin of the ground state is $S − N/2$ and the scattering of conduction electrons near the Fermi energy corresponds to *singular* Fermi liquid behavior.[19,20] Finally $2S < N$ corresponds to the *overscreened* Kondo effect, in which inelastic scattering persists even at vanishing temperatures and excitation energies, leading to a non-Fermi liquid. The simplest overscreened model is the two-channel Kondo one, $S = 1/2$, $N = 2$, in which the impurity contribution to the entropy is $\ln 2/2$ and the conductance per channel at low T has the form $G(T) \simeq G_0/2 \pm a\sqrt{T}$, where G_0 is the conductance at zero temperature in the one-channel case.[21,22]

The underscreened Kondo effect and quantum phase transitions involving partially Kondo screened spin-1 molecular states were observed in transport experiments by changing externally controlled parameters.[10,11] On the other hand, a system consisting in a Co atom inside a Au chain, in which the symmetry is reduced to four-fold by connecting it to appropriate leads, has been proposed as a possible realization of the overscreened Kondo model.[23–25] Here, the role of the two conduction channels is played by the $5d_{xz}$ and $5d_{yz}$ electrons of Au, which are equivalent by symmetry (asymmetry between the channels destroys the non-Fermi liquid behavior[22]).

We note that for one localized electron with two conduction channels equivalent by symmetry (for example xz and yz in tetragonal symmetry), one expects the orbital SU(2) symmetry, which combined with the spin SU(2) one leads to the SU(2) × SU(2) symmetry. However often in practice, the symmetry corresponds to a larger Lie group, the SU(4) one, leading to another exotic Kondo effect. In fact the low-energy

effective Hamiltonian for a molecule of iron(II) phtalocyanine on Au(111) has the SU(4) symmetry.[12,26] This is also the case for quantum dots in carbon nanotubes.[27–35] Recently, the SU(4) Kondo effect has been argued to correspond to experimental observations of a system of two quantum dots for a certain range of parameters.[7,36–41] As we show below, a Cu impurity in a Au chain doped with O can be described by the SU(4) Anderson model, which can be thought as a generalization of the Kondo model to include charge fluctuations. If instead of one we have two localized electrons, the Coulomb repulsion breaks the SU(4) symmetry. If in the system above the Cu impurity is replaced by Ni, the system can be described by a spin 1, two channel Kondo model with the SU(2) × SU(2) symmetry,[42] which is also analyzed in this work.

In this paper, we study the electronic structure of $3d$ impurities in oxygen doped gold chains. Using *ab initio* calculations, we determine the occupancy of the different spin-orbitals at the impurity site. In some problematic cases, we also use continuous-time quantum Monte Carlo with three orbitals to solve the impurity, in a similar way as in dynamical mean-field theory (DMFT). From this information, we infer the effective Anderson or Kondo model that describes the system at low energies. The case for a Co impurity[23–25] and a Ni one[42] was studied before. Using the numerical renormalization-group (NRG) applied to the effective model, we calculate explicitly the conductance as a function of temperature for the Ni impurity showing that it has a behavior qualitatively similar as for ordinary one-channel $S = 1/2$ Kondo impurities but with important and observable quantitative differences. We also calculate the conductance for a Cu impurity, corresponding to the SU(4) Anderson model.

In Section II we explain the different methods used in this work. Section III contains the results for the whole $3d$ series. In Section IV we summarize the results.

II. METHODS

The basis of this study consists in *ab initio* calculations based on density functional theory (DFT). We use the full potential linearized augmented plane waves method, as implemented in the WIEN2K code.[43] The generalized gradient approximation for the exchange and correlation potential in the parametrization of PBE (Perdew, Burke, and Ernzerhof),[44] and the augmented plane waves local orbital basis are used. The cutoff parameter, which gives the number of plane waves in the interstitial region, is taken as $R_{MT} * K_{max} = 7$, where K_{max} is the value of the largest reciprocal lattice vector used in the plane waves expansion and R_{MT} is the smallest muffin tin radius used. The number of **k** points in the Brillouin zone is enough, in each case, to obtain the desired energy and charge precisions, namely, 10^{-4} Ry and 10^{-4} e, respectively. In all the studied cases we consider a periodically repeated hexagonal lattice with $a = b = 15$ bohrs, and the coordinate system is fixed in such a way that the chain axis is aligned with z. The a and b distances in the supercell were checked to be large enough to avoid artificial interactions between the periodic replicas of the wire.

As it is known, transport experiments in Au chains indicate that the conduction channel is a single $6s$ band.[45,46] However,

due to self-interaction errors, DFT calculations can yield a spurious magnetization in a Au wire at its equilibrium distance, $d_{Au-Au}^{eq} = 4.9285$ bohrs.[47–49] In order to avoid it, we include a Hubbard $U = 4$ eV correction in the $5d$-electron Au manifold, as discussed in Ref. 42.

As mentioned in Section I, the purpose of this work is to study the Kondo physics in cases where the localized spin has magnitude S and can be screened by N channels, which correspond to conduction states of different symmetry. One possible experimental realization for obtaining the N channels in Au wires is the incorporation of O-dopants, which make the $5d_{xz,yz}$ orbitals of Au cross the Fermi level, due to the large hybridization with the oxygen $2p_{x,y}$ states, and the transfer of electrons to them due to the larger electronegativity of oxygen. In our previous work,[42] we have determined that an O-doping of 19% is the minimal amount needed in order to open the $|m| = 1$–symmetry conduction channel through all the Au atoms in the chain. The Au atoms that have an O atom as a nearest neighbor become slightly spin polarized. To avoid a magnetic interaction with the localized spin, in most of our calculations these Au atoms are placed away from the impurity.

In Fig. 1 we show a schematic representation of the 16-atom unit cell used in our *ab initio* calculations. The $3d$ impurity is placed in the center of the O-doped Au chain, and it has two O atoms symmetrically located as fourth neighbors. In this configuration, the effect of O-doping is the desired one and does not alter neither the spin-state nor the symmetries that each $3d$ impurity has when embedded in a bare Au chain. To set the distances between atoms in O-doped Au chains, we relax the Au–O distance for the case of AuO diatomic chain (two-atom unit cell) and, afterwards, we take the same bond length, $d_{Au-O}^{eq} = 3.625$ bohrs, for all the studied chains. In a similar way, we relax all the $3d$ impurity-Au distances taking into account the corresponding two-atom unit cell and fix the obtained length in the subsequent calculations.

Due to the presence of localized $3d$ electrons in a low dimensional system, we test the effects of electron correlations in the orbital occupancies, by including a variable Hubbard U parameter in the transition metal $3d$ orbitals. Among the different possibilities for the GGA+U approach, we use the self-interaction correction variant.[50] For some impurities, the spin state as well as the hole/electron's symmetry is stable when taking into account the correlations. However, there are a few cases (Cr and Fe) where GGA and GGA+U give qualitatively different results. In order to elucidate the charge distribution for those cases, we use the continuous-time quantum Monte Carlo (CTQMC).[52,53] For simplicity in these calculations we include only those orbitals which have a significant hybridization between the impurity and the rest of the chain, namely, those with angular momentum projection $m = \pm 1$ and $m = 0$. In all the treated cases, the states with $m = \pm 2$ are the most
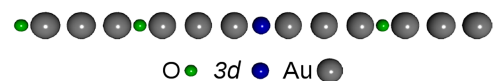

FIG. 1. Schematic representation of the unit cell used for the $3d$ impurity embedded in a 19% O-doped Au chain.

localized, as they lie perpendicular to the chain, thus having a small hybridization.

Restricting the Coulomb interaction to these states,[51] the effective Hamiltonian for the impurity takes the form

$$
\begin{aligned}
H_I = &\ U \sum_{\alpha} n_{\alpha,\uparrow} n_{\alpha,\downarrow} + J_t \sum_{\sigma_1,\sigma_2} d^{\dagger}_{xz,\sigma_1} d^{\dagger}_{yz,\sigma_2} d_{xz,\sigma_2} d_{yz,\sigma_1} \\
&+ J_t \sum_{\beta \neq \gamma} d^{\dagger}_{\beta,\uparrow} d^{\dagger}_{\beta,\downarrow} d_{\gamma,\downarrow} d_{\gamma,\uparrow} + (U - 2J_t) \sum_{\sigma_1,\sigma_2} n_{xz,\sigma_1} n_{yz,\sigma_2} \\
&+ (U - 2J_b) \sum_{\zeta} \sum_{\sigma_1,\sigma_2} n_{3z^2-r^2,\sigma_1} n_{\zeta,\sigma_2} \\
&+ J_b \sum_{\zeta} \sum_{\sigma_1,\sigma_2} d^{\dagger}_{3z^2-r^2,\sigma_1} d^{\dagger}_{\zeta,\sigma_2} d_{3z^2-r^2,\sigma_2} d_{\zeta,\sigma_1} \\
&+ J_b \sum_{\zeta} \left(d^{\dagger}_{3z^2-r^2,\uparrow} d^{\dagger}_{3z^2-r^2,\downarrow} d_{\zeta,\downarrow} d_{\zeta,\uparrow} + \text{H.c.} \right),
\end{aligned} \tag{1}
$$

where $d^{\dagger}_{\alpha,\sigma}$ ($d_{\alpha,\sigma}$) are creation (destruction) operators, $n_{\alpha,\sigma}$ the number operator, and the sum with α index runs over all orbitals ($3z^2 - r^2, xz, yz$) while the sums with other Greek index run over degenerate xz, yz symmetries. For an isolated impurity, we assume that the on-site energy of all $3d$ orbitals is the same. This neglects part of the crystal field due to interatomic Coulomb interactions, but this is usually much smaller than the effect of hopping with the neighbors which is included in our treatment.[51] For all cases we fix $U = 4$ eV, $J_t = 0.70$ eV, and $J_b = 0.49$ eV. The last two values result from a fit of the lowest atomic-energy levels of the $3d$ series. For a detailed discussion of the general values of these parameters, see Ref. 51.

The hybridization of the impurity with the Au-chains can be taken into account defining a hybridization matrix Δ which is simply related to the Green's function of the extreme site of the chain, close to the impurity. In Matsubara frequencies $i\omega_n = (2n - 1)\pi T$, with T the temperature in eV, it reads

$$
[\Delta(i\omega_n)]_{\alpha,\alpha} = t_{\alpha}^2 \left[G^0_L(i\omega_n) + G^0_R(i\omega_n) \right]_{\alpha,\alpha}. \tag{2}
$$

Here $G^0_{L(R)}$ are the Green's function of the nearest site to the left (right) of the impurity. They were obtained by first solving an isolated O-doped Au-chain with an empty site instead of a $3d$-impurity, by using GGA and then calculating the Green's function by definition, using the local density of states. The hopping parameters t_{α} were estimated from the fact that the imaginary part of the hybridization at zero frequency (after performing an analytic continuation), $\Gamma_{\alpha} = -\mathcal{I}m\Delta(0)_{\alpha,\alpha} = \pi t_{\alpha}^2(\rho_L(0) + \rho_R(0))$, can be related with the half-width of the peak corresponding to the GGA $3d$-impurity density of states. For the studied cases of Cr and Fe, we obtain $t_{3z^2-r^2} = 0.38$ eV, while $t_{xz,yz} = 0.7$ eV for Cr and $t_{xz,yz} = 1.05$ eV for Fe. It might seem surprising that $t_{3z^2-r^2} < t_{xz,yz}$ since the hopping between two d orbitals with $m = 0$ is expected to be larger than the corresponding hopping for $m = \pm 1$. However, the relevant parameter is Γ_{α}, and it is always larger for $\alpha = 3z^2 - r^2$.

The impurity (1) and its hybridization with the chains (2) define an effective multiorbital Anderson model that can be solved by continuous time quantum Monte Carlo. Here we use a hybridization expansion based algorithm.[52,54]

As we will show in Sec. III, for the Cr impurity we fix its total occupancy to two electrons while for Fe we considered two cases with total occupancies of three and four electrons.

To calculate the conductance in specific cases, we use the numerical renormalization group[55,56] as implemented in the NRG Ljubljana open source code.[57,58] We take the discretization parameter $\Lambda = 3$ and we keep up to 10 000 states.

III. RESULTS

In Table I we present the *ab initio* results for the orbital projected electronic occupancies obtained integrating the charge in each muffin tin, for the first five members of the $3d$ series, when considering $U = 0$ at the impurity sites. The effect of U is discussed below. We note that the *ab initio* methods discussed in Sec. II are mean-field approximations and predict a long-range ferromagnetic order, which is not expected in a one dimensional system. This has been proved, for example, for the periodic Anderson model.[59] In spite of this, we believe that the predicted charge distribution for the magnetic impurity is in general reliable for a given orientation of the spin of the Hund rules ground state and consistent with CTQMC, which does not break the SU(2) symmetry.

From the resulting occupancies, we expect the following behavior for the different impurities:

A. Sc

This case should correspond to only one electron at the impurity site. The obtained partial occupancies indicate that this electron occupies one of the degenerate orbitals $d_{x^2-y^2}$, d_{xy}. Since the top of the Au states with the same symmetry lies about 1.3 eV below the Fermi energy, the states with one of these orbitals occupied have practically no hybridization with the Au states. Thus one expects a localized spin 1/2 and no Kondo effect. The mixing with other configurations suggested by the occupancies of Table I is probably an artifact of the GGA.

B. Ti

One electron occupies one of the degenerate orbitals $d_{x^2-y^2}$, d_{xy}, and another one partially occupies the $d_{3z^2-r^2}$ orbital. One can describe the system as valence fluctuations between a configuration with one "frozen" electron (because it has no hopping) with $|m| = 2$ and another one with two electrons (the other electron occupying the $d_{3z^2-r^2}$ orbital) with spin 1 due to Hund's rules. This model was solved exactly

TABLE I. Orbital projected electronic occupancies for majority spin for the different elements. All the minority spin d orbitals are almost empty.

$3d$ impurity	$n(3d_{3z^2-r^2} \uparrow)$	$n(3d_{xy,x^2-y^2} \uparrow)$	$n(3d_{xz,yz} \uparrow)$
Sc	0.12	0.31	0.13
Ti	0.43	0.99	0.16
V	0.77	1.64	0.21
Cr	0.80	1.72	1.23
Mn	0.91	1.86	1.86

by Bethe ansatz.[60–63] The physics corresponds to that of the underscreened $S = 1$, one-channel Kondo model.

C. V

Two electrons occupy each of the inert orbitals $d_{x^2-y^2}$, d_{xy} with majority spin. A third electron fluctuates between the localized $d_{3z^2-r^2}$ orbital at V and the Au band with the same symmetry. The occupancy of the V $3d_{3z^2-r^2}$ orbital is high suggesting that the model that describes the system is the $S = 3/2$ one-channel Kondo one. If charge fluctuations are important, the model that describes the system is the one that mixes the $S = 3/2$ configuration with the two-electron $S = 1$ one. This model is also exactly solvable.[61–63] The ground state has total spin 1 and therefore corresponds to the underscreened case.

D. Cr

As for V, the inert orbitals with majority spin are occupied. In addition, it seems that there is a little bit less than one electron in the $d_{3z^2-r^2}$ orbital and a little bit more than one electron in the degenerate orbitals d_{xz} and d_{yz}. Assuming integer occupancies, one has an orbitally degenerate $S = 2$ impurity screened by three channels. One would expect a two-stage partial screening, first by the $5d_{3z^2-r^2}$ Au conduction states which have a larger hybridization and then by the $5d_{xz}$ and $5d_{yz}$, with some similarities to iron(II) phtalocyanine molecules on Au(111),[12] but here the ground state would have $S = 1$.

In order to study in more detail the charge distribution between the hybridized orbitals with $|m| < 2$, we have performed GGA+U calculations introducing the interaction U in the $3d$ shell. We have to mention that in the case of V no appreciable changes are seen when U is introduced. For this reason we omit the details for V. Instead, from Fig. 2, we see that the effect of U for Cr is to push up the $3d_{3z^2-r^2}$ orbital and transfer the electron to the $|m| = 1$ orbitals. This is more clearly seen in Table II where the partial occupancies are shown. The results for $U = 4$ eV suggest a ground state with all orbitals with $|m| > 0$ occupied forming an $S = 2$ orbitally
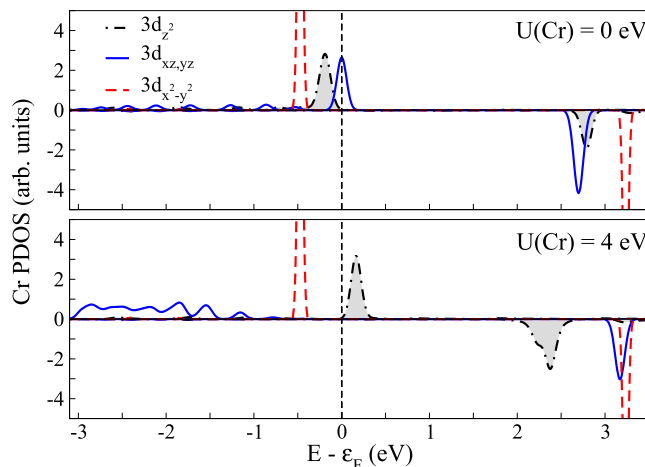

FIG. 2. Partial density of states for the Cr impurity embedded in an O-doped gold chain with $U = 0$ (top) and $U = 4$ eV (bottom) at the impurity site.

TABLE II. Orbital projected electronic occupancies of the Cr majority spin for different values of U at the Cr site.

U (eV)	$n(3d_{3z^2-r^2} \uparrow)$	$n(3d_{xy,x^2-y^2} \uparrow)$	$n(3d_{xz,yz} \uparrow)$
0	0.80	1.72	1.23
2	0.82	1.73	1.27
3	0.20	1.76	1.75
4	0.15	1.77	1.77

non-degenerate ground state screened by two degenerate channels ($m = \pm 1$).

In attempt to clarify the discrepancies in the charge distribution as a function of U in the GGA+U calculation, we have used CTQMC as outlined in Sec. II. We assume that one electron occupies each of the inert orbitals $m = \pm 2$, with parallel spins, and adjust the chemical potential in such a way that two additional electrons are present in the system formed by the other orbitals with $|m| < 2$, the interactions among which is described by Eq. (3). The resulting charge distribution indicates that these two additional electrons occupy each of the $|m| = 1$ orbitals. This distribution agrees with GGA+U for large U. In spite of the complexity introduced by the presence of two channels, we expect a similar physics to the one-channel $S > 1/2$ underscreened Kondo model, with singular Fermi liquid behavior.

E. Mn

As expected, this case corresponds to an $S = 5/2$ Kondo model, partially screened by the three conduction channels ($|m| < 2$) at low enough temperatures.

In Table III we list the orbital projected electronic occupancies for the remaining members of the $3d$ series, except for Zn, which is expected to have a full $3d$ shell and therefore not showing interesting physics. In all the listed cases we consider $U = 0$ at the impurity sites.

F. Fe

It has six electrons, or four holes in the $3d$ shell. The GGA results point to 1.40 holes in the inert $|m| = 2$ orbitals, 0.81 holes in the $m = 0$ one, and 1.61 holes in the $|m| = 1$ orbitals. However, since the $|m| = 2$ electrons do not hop, one expects an integer population of them. If the occupancy is 1 and the remaining 3 holes occupy each of the remaining orbitals ($d_{3z^2-r^2}, d_{xz}, d_{xz}$), the configuration is similar to that of Co below except for the presence of the $3d_{3z^2-r^2}$ hole. Interestingly after a first-stage Kondo effect in which the spin of this orbital is screened (as in iron(II) phtalocyanine on Au(111)[12]), the physics would be the same as that for a Co impurity (discussed below).

TABLE III. Orbital projected electronic occupancies for the minority spin for the different elements. All the majority spin d orbitals are occupied.

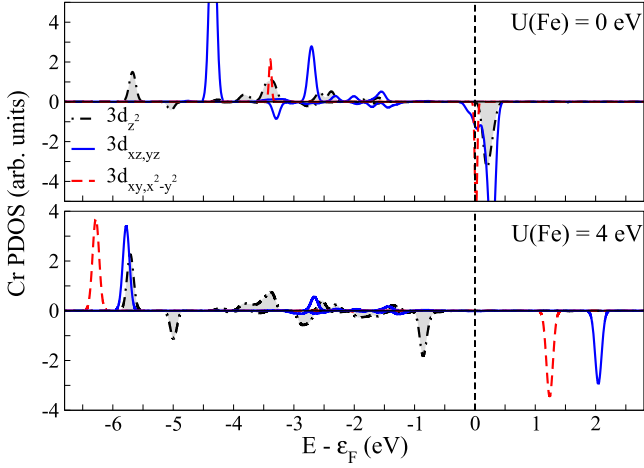| Case	$n(3d_{3z^2-r^2} \downarrow)$	$n(3d_{xy,x^2-y^2} \downarrow)$	$n(3d_{xz,yz} \downarrow)$
Fe	0.19	0.60	0.39
Co	0.88	1.17	0.22
Ni	0.92	1.87	0.56
Cu	0.83	1.89	1.87

FIG. 3. Partial density of states for the Fe impurity embedded in an O-doped gold chain with $U = 0$ (top) and $U = 4$ eV (bottom) at the impurity site.

In this case, we have also investigated the effect of U within GGA+U to gain more insight into the charge distribution. Taking into account the results shown in Fig. 3 and the occupancies listed in Table IV, we see here that the effect of U is to push down the $d_{3z^2-r^2}$ orbital, increasing abruptly its occupancy between $U = 2$ eV and $U = 3$ eV. In this case, all holes are in $3d$ states with $|m| > 0$. By an electron-hole transformation, the physics is the same as that suggested by GGA+U for large U for Cr: an $S = 2$ orbitally non-degenerate ground state screened by two degenerate channels.

As for the case of Cr, we have studied the charge distribution with CTQMC. In this case we have the additional ambiguity that the occupancy of the inert orbitals, absent in the Hamiltonian solved by CTQMC, lies between 2 and 3, for a total occupancy of 6 electrons. Therefore we have adjusted the chemical potential in this Hamiltonian for two occupancies: (i) 4 and (ii) 3 electrons. In the first case we obtain a double occupancy of the $3d_{3z^2-r^2}$ and single occupancy of the $m = \pm 1$ orbitals, in agreement with Table IV for large U. In case (ii) we obtain one electron in each of the non-inert orbitals ($d_{3z^2-r^2}$, d_{xz}, d_{xz}), resulting in the Co configuration with an additional $3d_{3z^2-r^2}$ hole, mentioned above. Unfortunately our results are not enough to determine which of these two configurations is more probable.

G. Co

As shown before,[23] the configuration of Co corresponds to two holes occupying the $|m| = 1$ orbitals and the remaining one is in one of the inert $|m| = 2$ orbitals, forming a total spin $S = 3/2$ according to Hund's rules. There is some admixture

with the $S = 1$ ground-state configuration of Ni described below. The low temperature physics corresponds to an under-screened Kondo model, $S = 3/2$ screened by two channels. It is interesting that under an appropriate tetragonal crystal field, the orbital degeneracy of the $|m| = 2$ orbitals is broken and at the same time the spin-orbit coupling leads to a physics similar to the $S = 1/2$ two-channel Kondo model with non-Fermi liquid properties. This has been discussed in detail elsewhere.[23–25] As stated above, Fe impurities might display similar physics.

H. Ni

From the occupancies listed in Table III, one realizes that Ni fluctuates between a configuration with two holes and total spin 1 in the degenerate orbitals with $|m| = 1$ and one with one hole in one of these orbitals. A closer investigation of the effective model reported before indicates that the first configuration dominates and the system is in the Kondo regime.[42] This is confirmed by our NRG calculations on the effective model H_{eff}. Thus the system can be considered as a realization of a two-channel fully screened $S = 1$ Kondo model. The effective Hamiltonian including charge fluctuations is[42]

$$H_{eff} = \sum_{M_2}(E_2 + DM_2^2)|M_2\rangle\langle M_2| + \sum_{\alpha M_1}E_1|\alpha M_1\rangle\langle\alpha M_1|$$
$$+ \sum_{\nu k\alpha\sigma}\epsilon_{\nu k}c_{\nu k\alpha\sigma}^{\dagger}c_{\nu k\alpha\sigma} + \sum_{M_1 M_2}\sum_{\alpha\nu k\sigma}V_{\nu\alpha}\langle 1M_2|\frac{1}{2}\frac{1}{2}M_1\sigma\rangle$$
$$\times (|M_2\rangle\langle\alpha M_1|c_{\nu k\alpha\sigma} + \text{H.c.}), \qquad (3)$$

where E_i and M_i indicate the energies and the spin projections along the chain, chosen as the quantization axis, of states with $i = 1, 2$ holes in the $3d$ shell of the Ni impurity, and $c_{\nu k\alpha\sigma}^{\dagger}$ creates a hole in the conduction band with symmetry α and spin σ at the left or right of the impurity (denoted by the subscript ν) with wave vector k.
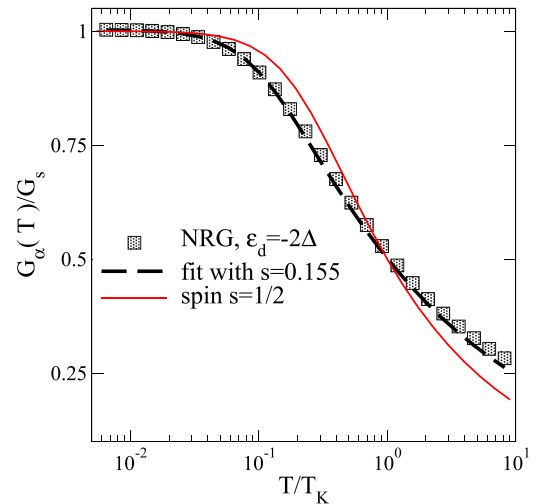

FIG. 4. Squares: NRG data for $G_{\alpha}(T) = \sum_{\sigma} G_{\alpha\sigma}(T)$ in units of its maximum G_s as a function of T/T_K for $\epsilon_d = -2\Delta$, where $\Delta = 0.115$ eV is half the resonant-level width.[42] Dashed black line: fitting of numerical data with expression Eq. (4) with $s = 0.155$. Continuous red line: Eq. (4) with $s = 0.22$.

TABLE IV. Orbital projected electronic occupancies of the Fe minority spin for different values of U at the Fe site.

U(Fe) (eV)	$n(3d_{3z^2-r^2}\downarrow)$	$n(3d_{xy,x^2-y^2}\downarrow)$	$n(3d_{xz,yz}\downarrow)$
0	0.19	0.60	0.39
2	0.16	0.69	0.23
3	0.89	0.01	0.13
4	0.89	0.01	0.11

TABLE V. Symmetry-dependent d-band minority spin fillings of the Cu atoms (in electrons) for the selected studied cases. The color coding of the schematic representation of the chains is the one presented in Fig. 1.

Case	$n(3d_{3z^2-r^2}\downarrow)$	$n(3d_{xy,x^2-y^2}\downarrow)$	$n(3d_{xz,yz}\downarrow)$
	0.83	1.89	1.87
	0.91	1.89	1.64
	0.90	1.89	1.65
	0.83	1.79	1.36

The ground state of this model is a Fermi liquid, as for the one-channel $S = 1/2$ Kondo model. The reader might ask if there are important differences in the properties of both models. One difference is that well inside the Kondo regime, the conductance at zero temperature is two times larger in the two-channel $S = 1$ case ($4e^2/h$ for symmetric contacts) because two conduction channels and two spins are contributing. Experimentally, asymmetry between the couplings of the impurity to the left and the right decreases the conductance, but this difference is likely observable in real experiments. Another difference is that the *shape* of the conductance as a function of temperature is different in the two cases. This is shown in Fig. 4, where the conductance is calculated for the parameters extracted in Ref. 42. For the one-channel $S = 1/2$ Anderson model, it is well known that the empirical expression

$$G(T) = \frac{G_s}{\left[1 + \left(2^{1/s} - 1\right)(T/T_K)^2\right]^s},\tag{4}$$

where $s = 0.22$ and G_s is the conductance at temperature $T = 0$, matches not only the experimental results but also NRG calculations.[1,64] For the parameters that we extract for Ni in O-doped Au chains, we obtain that a similar empirical law holds but with $s = 0.155$, yielding a less steep decrease in the intermediate temperature regime.

I. Cu

Since Cu is similar to Au, it has an almost filled $3d$ shell, and therefore oxygen doping moves the spectral density of the orbitals with $|m| = 1$ to the Fermi energy, introducing a partial emptying of these orbitals.[24] We analyze the effect of the presence of oxygen impurities on the spin-state of the Cu impurity or its hole's symmetries, for several configurations, also changing the amount of O in the Au chain. In Table V we introduce the different cases studied and their corresponding Cu occupancy numbers (in electrons) obtained by integrating the minority band separated in the different symmetries, within the Cu-muffin-tin sphere. From the last configuration listed in Table V, it can be inferred that for this case a hole of the Au–O conduction bands with symmetry either xz or yz and spin either up or down can enter the full $3d$ shell of Cu or vice versa. Thus, this system can be described by an SU(4) Anderson model.[12,26]

In Fig. 5 we show the NRG result for the total conductance $G(T)$ as a function of temperature in units of $G_0 = 2e^2/h$ for

three values of the on-site energy of the xz and yz orbitals relative to the Fermi energy, ϵ_d, and hybridization $\Delta = 0.01$ in units of the half-bandwidth D. All of them correspond to the intermediate valence regime with a total occupancy of the $3d$ shell of 0.484 for $\epsilon_d = -3\Delta$, 0.439 for $\epsilon_d = -2.5\Delta$, and 0.398 for $\epsilon_d = -2\Delta$, shared equally between the four spin-orbitals. Note that the intermediate-valence regime in the present SU(4) case extends to larger values of $-\epsilon_d/\Delta$ than in the most usual SU(2) case. There is a clear maximum at temperatures of the order of ϵ_d. At smaller temperatures, the conductance is rather flat, in contrast to other fully screened cases, such as those displayed in Fig. 4.

At $T = 0$ the conductance is determined by the Friedel sum rule. For constant density of states and hybridization (as we have assumed for the NRG results), according to this rule, the contribution of the conductance for each spin and channel with occupancy $n_{\alpha\sigma}$ is[40]

$$G_{\alpha\sigma} = \frac{e^2}{h}\sin^2(\pi n_{\alpha\sigma}),\tag{5}$$

and $G = \sum_{\alpha\sigma} G_{\alpha\sigma}$.

The numerical results of Fig. 5 are quite consistent with this rule. They lie above those obtained using Eq. (5) by near 1%. This is likely due to numerical errors in the conductance.
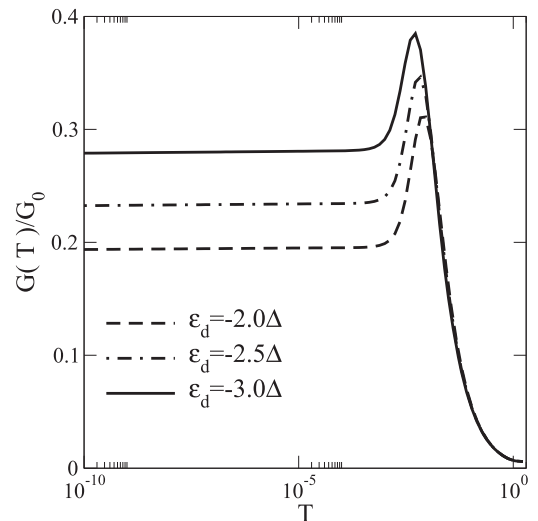

FIG. 5. Total NRG conductance $G(T)$ for the SU(4) Anderson model as a function of temperature, for three values of ϵ_d (-2Δ, -2.5Δ, and -3Δ) with hybridization $\Delta = 0.01$ in units of the half-bandwidth D.

IV. SUMMARY AND DISCUSSION

Using *ab initio* methods combined with continuous-time quantum Monte Carlo, we have studied the electronic structure of systems with one substitutional $3d$ impurity in oxygen doped gold chains, along the whole $3d$ series, searching for unusual behavior in the screening of the impurity spin. The effect of oxygen doping is to bring $5d_{xz}$ and $5d_{yz}$ orbitals to the Fermi energy, which together with the $5d_{3z^2-r^2}$ ones constitute three screening channels for the impurity spin.

We left Zn out because one expects that it has a full $3d$ shell and no magnetism. At the other end of the $3d$ series, we find that Sc behaves as an isolated magnetic impurity with spin $S = 1/2$, because it has one electron occupying either the $3d_{x^2-y^2}$ or the $3d_{xy}$ orbitals, and they have a negligible hybridization with the orbitals of the rest of the chain. For this reason we call them inert.

The system with Ni and Cu impurities behaves as a Fermi liquid, obeying the Friedel sum rule. In the first case, the low-energy physics can be described by a fully compensated $S = 1$, two-channel Kondo model. In this case, we have calculated the conductance through the system using NRG, pointing out quantitative differences with the most usual $S = 1/2$, one-channel case. For Cu impurities, the appropriate low-energy model is the SU(4) Anderson impurity one, in the intermediate-valence regime. In this case, the conductance also shows differences with more usual cases.

The remaining systems, taking out some peculiarities, are expected to behave as singular Fermi liquids, like underscreened Kondo model. This is due to the presence of partially filled inert orbitals which tend to couple into large spins due to the Hund rules and cannot be screened by the conduction electrons. The conductance as a function of temperature for several underscreened Kondo models is presented in the Supplementary material of Ref. 10. Particularly complex is the case of Cr, in which different configurations seem mixed, and Fe, for which our results are inconclusive with respect of the ground state configuration. One possibility for Fe is that it has the same configuration of Co with one additional $3d_{x^2-y^2}$ hole. The spin of this hole is expected to be screened in a first-stage Kondo effect leaving a low-energy physics similar to that of Co. As shown before for the latter,[23–25] under an appropriate tetragonal crystal field, which can be realized connecting the system with leads with a square cross section, the spin-orbit coupling leads to an effective spin 1/2 overscreened by two degenerate channels with xz and yz symmetries, leading to non-Fermi-liquid behavior.

The results using CTQMC have been done using a restricted basis set. This has the advantage of accelerating the time in the calculations, and the interactions take a simpler form than those of the complete basis set.[51] The main drawback however is then the Hund interaction with the spin of the inert orbitals is neglected. We believe that this does not alter the resulting occupancies of Cr and Fe because the resulting spin of the remaining orbitals is the maximum possible, taking maximum advantage of the Hund interaction.

Finally we comment on the effect of symmetry-breaking perturbations, like distortions or defects in the chains. This effect breaks the channel degeneracy and changes the physics in those cases in which the impurity has partial degenerate orbitals which are not inert. For example in the case of Ni, breaking of the degeneracy of the xz and yz orbitals would change the $S = 1$ two-channel Kondo physics, in a two-stage Kondo model with two characteristic temperatures, each one corresponding to each channel. The ground-state however continues to be a Fermi liquid. In the case of Co, the partial screening of the $S = 3/2$ spin by two channels also would occur in two stages, but the ground state still corresponds to an $S = 1/2$ singular Fermi liquid. The breaking of symmetry is more dramatic for Co in tetragonal symmetry because the symmetry breaking renders the effective $S = 1/2$ overscreened model with non-Fermi liquid behavior to a usual Fermi liquid below a characteristic energy scale. A previous estimate indicates that this scale is below T_K (and the non-Fermi liquid features are observable) if the splitting between xz and yz orbitals is less than 100 meV.[23]

[1] D. Goldhaber-Gordon, H. Shtrikman, D. Mahalu, D. Abusch-Magder, U. Meirav, and M. A. Kastner, Nature **391**, 156 (1998).
[2] S. M. Cronenwet, T. H. Oosterkamp, and L. P. Kouwenhoven, Science **281**, 540 (1998).
[3] D. Goldhaber-Gordon, J. Göres, M. A. Kastner, H. Shtrikman, D. Mahalu, and U. Meirav, Phys. Rev. Lett. **81**, 5225 (1998).
[4] W. G. van der Wiel, S. de Franceschi, T. Fujisawa, J. M. Elzerman, S. Tarucha, and L. P. Kowenhoven, Science **289**, 2105 (2000).
[5] M. Grobis, I. G. Rau, R. M. Potok, H. Shtrikman, and D. Goldhaber-Gordon, Phys. Rev. Lett. **100**, 246601 (2008), references therein.
[6] S. Amasha, A. J. Keller, I. G. Rau, A. Carmi, J. A. Katine, H. Shtrikman, Y. Oreg, and D. Goldhaber-Gordon, Phys. Rev. Lett. **110**, 046604 (2013).
[7] A. J. Keller, S. Amasha, I. Weymann, C. P. Moca, I. G. Rau, J. A. Katine, H. Shtrikman, G. Zaránd, and D. Goldhaber-Gordon, Nat. Phys. **10**, 145 (2014).
[8] S. Kubatkin, A. Danilov, M. Hjort, J. Cornil, J. L. Brédas, N. Stuhr-Hansen, P. Hedegård, and Th. Björnholm, Nature **425**, 699 (2003).
[9] J. J. Parks, A. R. Champagne, G. R. Hutchison, S. Flores-Torres, H. D. Abruña, and D. C. Ralph, Phys. Rev. Lett. **99**, 026601 (2007).
[10] J. J. Parks, A. R. Champagne, T. A. Costi, W. W. Shum, A. N. Pasupathy, E. Neuscamman, S. Flores-Torres, P. S. Cornaglia, A. A. Aligia, C. A. Balseiro, G. K.-L. Chan, H. D. Abruña, and D. C. Ralph, Science **328**, 1370 (2010).
[11] S. Florens, A. Freyn, N. Roch, W. Wernsdorfer, F. Balestro, P. Roura-Bas, and A. A. Aligia, J. Phys.: Condens. Matter **23**, 243202 (2011), references therein.
[12] E. Minamitani, N. Tsukahara, D. Matsunaka, Y. Kim, N. Takagi, and M. Kawai, Phys. Rev. Lett. **109**, 086602 (2012).
[13] H. Ohnishi, Y. Kondo, and K. Takayanagi, Nature **395**, 780 (1998).
[14] R. H. M. Smit, C. Untiedt, A. I. Yanson, and J. M. van Ruitenbeek, Phys. Rev. Lett. **87**, 266102 (2001).
[15] V. Rodrigues, J. Bettini, P. C. Silva, and D. Ugarte, Phys. Rev. Lett. **91**, 096801 (2003).
[16] A. Enomoto, S. Kurokawa, and A. Sakai, Phys. Rev. B **65**, 125410 (2002).
[17] D. J. Bakker, Y. Noat, A. I. Yanson, and J. M. van Ruitenbeek, Phys. Rev. B **65**, 235416 (2002).
[18] A. C. Hewson, *The Kondo Problem to Heavy Fermions* (Cambridge University Press, 1993).
[19] P. Mehta, N. Andrei, P. Coleman, L. Borda, and G. Zaránd, Phys. Rev. B **72**, 014430 (2005).
[20] D. E. Logan, C. J. Wright, and M. R. Galpin, Phys. Rev. B **80**, 125117 (2009).

[21] G. Zaránd, C.-H. Chung, P. Simon, and M. Vojta, Phys. Rev. Lett. **97**, 166802 (2006).

[22] A. K. Mitchell, A. K. Sela, and D. E. Logan, Phys. Rev. Lett. **108**, 086405 (2012).

[23] S. Di Napoli, A. Weichselbaum, P. Roura-Bas, A. A. Aligia, Y. Mokrousov, and S. Blügel, Phys. Rev. Lett. **110**, 196402 (2013).

[24] S. Di Napoli, M. A. Barral, P. Roura-Bas, A. A. Aligia, Y. Mokrousov, and A. M. Llois, IEEE Trans. Magn. **49**, 4683 (2013).

[25] S. Di Napoli, P. Roura-Bas, A. Weichselbaum, and A. A. Aligia, Phys. Rev. B **90**, 125149 (2014).

[26] J. Fernández, A. A. Aligia, and A. M. Lobos, Europhys. Lett. **109**, 37011 (2015), references therein.

[27] P. Jarillo-Herrero, J. Kong, H. S. J. van der Zant, C. Dekker, L. P. Kouwenhoven, and S. De Franceschi, Nature **434**, 484 (2005).

[28] M.-S. Choi, R. López, and R. Aguado, Phys. Rev. Lett. **95**, 067204 (2005).

[29] J. S. Lim, M.-S. Choi, M. Y. Choi, R. López, and R. Aguado, Phys. Rev. B **74**, 205119 (2006).

[30] F. B. Anders, D. E. Logan, M. R. Galpin, and G. Finkelstein, Phys. Rev. Lett. **100**, 086809 (2008).

[31] S. Lipinski and D. Krychowski, Phys. Rev. B **81**, 115327 (2010).

[32] C. A. Büsser, E. Vernek, P. Orellana, G. A. Lara, E. H. Kim, A. E. Feiguin, E. V. Anda, and G. B. Martins, Phys. Rev. B **83**, 125404 (2011).

[33] L. Tosi, P. Roura-Bas, and A. A. Aligia, Physica B **407**, 3259 (2012).

[34] K. Grove-Rasmussen, S. Grap, J. Paaske, K. Flensberg, S. Andergassen, V. Meden, H. I. Jorgensen, K. Muraki, and T. Fujisawa, Phys. Rev. Lett. **108**, 176802 (2012).

[35] P. Roura-Bas, L. Tosi, A. A. Aligia, and P. S. Cornaglia, Phys. Rev. B **86**, 165106 (2012).

[36] L. Tosi, P. Roura-Bas, and A. A. Aligia, Phys. Rev. B **88**, 235427 (2013).

[37] Y. Nishikawa, A. C. Hewson, D. J. G. Crow, and J. Bauer, Phys. Rev. B **88**, 245130 (2013).

[38] M. Filippone, C. P. Moca, G. Zaránd, and C. Mora, Phys. Rev. B **90**, 121406(R) (2014).

[39] Z. Q. Bao, A. M. Guo, and Q. F. Sun, J. Phys.: Condens. Matter **26**, 435301 (2014).

[40] L. Tosi, P. Roura-Bas, and A. A. Aligia, J. Phys.: Condens. Matter **27**, 335601 (2015).

[41] Y. Nishikawa, O. J. Curtin, A. C. Hewson, D. J. G. Crow, and J. Bauer, Phys. Rev. B **93**, 235115 (2016).

[42] S. Di Napoli, M. A. Barral, P. Roura-Bas, L. O. Manuel, A. M. Llois, and A. A. Aligia, Phys. Rev. B **92**, 085120 (2015).

[43] P. Blaha, K. Schwarz, G. K. H. Madsen, D. Kvasnicka, and J. Luitz, *WIEN2k: An Augmented Plane Wave+Local Orbitals Program for Calculating Crystal Properties* (TU Wien, Wien, Austria, 2001).

[44] J. P. Perdew, S. Burke, and M. Ernzerhof, Phys. Rev. Lett. **77**, 3865 (1996).

[45] G. C. Rego, A. R. Rocha, V. Rodrigues, and D. Ugarte, Phys. Rev. B **67**, 045412 (2003).

[46] N. Agraït, A. L. Yeyati, and J. M. van Ruitenbeek, Phys. Rep. **377**, 81 (2003).

[47] Y. Miura, R. Mazzarello, A. Dal Corso, A. Smogunov, and E. Tosatti, Phys. Rev. B **78**, 205412 (2008).

[48] P. Lucignano, R. Mazzarello, A. Smogunov, M. Fabrizio, and E. Tosatti, Nat. Mater. **8**, 563 (2009).

[49] G. Sclauzero and A. Dal Corso, Phys. Rev. B **87**, 085108 (2013).

[50] I. Anisimov, I. V. Solovyev, M. A. Korotin, M. T. Czyzyk, and G. A. Sawatzky, Phys. Rev. B **48**, 16929 (1993).

[51] A. A. Aligia and T. Kroll, Phys. Rev. B **81**, 195113 (2010).

[52] P. Werner, A. Comanac, L. De Medici, M. Troyer, and A. J. Millis, Phys. Rev. Lett. **97**, 076405 (2006).

[53] K. Haule, Phys. Rev. B **75**, 155113 (2007).

[54] E. Gull, A. J. Millis, A. I. Lichtenstein, A. N. Rubtsov, M. Troyer, and P. Werner, Rev. Mod. Phys. **83**, 349 (2011).

[55] K. G. Wilson, Rev. Mod. Phys. **47**, 773 (1975).

[56] H. R. Krishna-murthy, J. W. Wilkins, and K. G. Wilson, Phys. Rev. B **21**, 1003 (1980); **21**, 1044 (1980).

[57] R. Žitko, NRG Ljubljana—Open source numerical renormalization group code, http://nrgljubljana.ijs.si, 2014.

[58] R. Žitko and T. Pruschke, Phys. Rev. B **79**, 085106 (2009).

[59] C. Noce and M. Cuoco, Phys. Rev. B **59**, 7409 (1999).

[60] A. A. Aligia, C. R. Proetto, and C. A. Balseiro, Phys. Rev. B **31**, 6143(R) (1985).

[61] A. A. Aligia, C. A. Balseiro, and C. R. Proetto, Phys. Rev. B **33**, 6476 (1986).

[62] A. A. Aligia, C. A. Balseiro, C. R. Proetto, and P. Schlottmann, Z. Phys. B **62**, 311 (1986), references therein.

[63] A. A. Aligia, C. A. Balseiro, C. R. Proetto, and P. Schlottmann, J. Magn. Magn. Mater. **63-64**, 231 (1987).

[64] T. A. Costi, Phys. Rev. Lett. **85**, 1504 (2000).